

www.acsami.org Research Article

Holistic Design Consideration of Metal—Organic Framework-Based Composite Membranes for Lithium—Sulfur Batteries

Dong Ju Lee, Xiaolu Yu, R. Eric Sikma, Mingqian Li, Seth M. Cohen, Guorui Cai,* and Zheng Chen*



Cite This: ACS Appl. Mater. Interfaces 2022, 14, 34742-34749



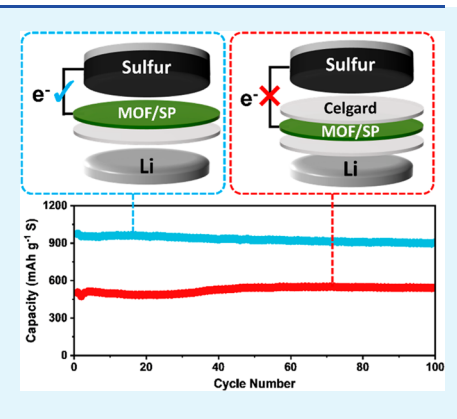
ACCESS

III Metrics & More

Article Recommendations

Supporting Information

ABSTRACT: Metal—organic framework (MOF)-based membranes have received significant attention as separators for lithium—sulfur (Li–S) batteries because of their high porosities, well-defined and tailored structures, and other tunable features that are desirable for preventing the "shuttle effect" of soluble polysulfides. Because of the insulating nature of most MOFs, composite membranes are generally constructed by a combination of MOFs and electron-conductive materials. In this work, we examine the property—performance relation between MOF-based separators and Li–S batteries by systematically adjusting the electrical conductivity, thickness, and mass loading of the MOF-based composite. Beyond the commonly referenced trapping or blocking ability of MOFs toward polysulfides, we find that by fixing the thickness of the MOF-based composite coating layer (\sim 40 μ m) on a Celgard membrane, the electrical conductivity of the MOF composite layer is of paramount importance compared with the physical/chemical trapping ability of polysulfides. However, the trapping ability of MOFs becomes indispensable when the thickness of the composite layer is small (e.g., \sim 20



μm), indicating the synergetic effects of the adsorption and conversion capabilities of the thin composite layer. This work suggests the importance of a holistic design consideration for a MOF-based membrane for long-life and high-energy-density Li–S batteries. KEYWORDS: metal-organic frameworks (MOFs), lithium-sulfur (Li–S) battery, shuttle effect, polysulfide, adsorption, conductivity

1. INTRODUCTION

Lithium-sulfur (Li-S) batteries have been considered as potential next-generation energy storage devices because of their high energy density (2600 Wh kg⁻¹), as well as the natural abundance and low environmental footprint of sulfur. 1-4 However, the practical application of Li-S batteries is impeded by the "shuttle effect" caused by the migration of soluble reaction intermediates, lithium polysulfide (LiPS, Li₂S_n, $4 \le n \le 8$) species, which dissolve in the electrolyte and diffuse across the separator to the lithium anode. The diffused LiPS species then undergo a parasitic reaction and deposit Li₂S/ Li₂S₂ on the lithium anode surface, leading to the loss of active material, corrosion of the lithium anode, consumption of the electrolyte, and decreased Coulombic efficiency. 5-9 Studies to address these issues have focused on modifying the commercial separators with nanoporous materials to block or trap the diffusion of LiPS species. 9–14 Among many candidate materials that have been studied are carbon-based materials, metal oxides, and metal-organic frameworks (MOFs), the latter of which have been widely investigated because of their high porosities and well-defined, tunable pore sizes. $^{15-20}$

Despite the improved cycling performance of Li–S batteries by using MOF-modified separators, ^{21–23} the trapped LiPS species within the MOF pores are difficult to reutilize for subsequent cycling because of the insulating nature of most MOFs, thereby leading to an irreversible loss of the cycling

capacity. ^{24,25} To overcome this issue, researchers have mixed MOFs with conductive materials to provide electron pathways, so that the trapped LiPS species in the separator can be more effectively reutilized during the repeating charging/discharging process. ^{26–30} Although many of the previous studies attribute the improved performance to the physical/chemical blocking and trapping effect of MOFs toward LiPS species, ^{27,30,31} the underlying mechanism of how each component and their interplay in the composite influences the battery performance is still unclear.

In this work, we reconsider the property–performance relation between MOF-based composite separators and Li–S batteries by systematically adjusting the electrical conductivity of the MOF-based composite coating layer. UiO-66-NH₂ (UiO = University of Oslo), a Zr(IV)-based MOF, was adopted as a model material to design and fabricate MOF-based composite separators with tunable electrical conductivity. UiO-66-NH₂ powder was mixed with Super P (SP) carbon black and polymer binder at different ratios and cast on a commercial

Received: May 12, 2022 Accepted: July 17, 2022 Published: July 25, 2022





Celgard 2500 membrane with controlled thicknesses (~40 μ m) of the coating layer. Using the composite layer (MOF/ SP) modified Celgard as the separator, Li-S half cells were assembled for long-term cycling and rate capability tests, which showed that the cycling performance was strongly correlated with the electrical conductivity of the MOF/SP layer. The composite coating layers with higher SP content show improved initial capacity, capacity retention, and lower overpotential, which is primarily due to the increased sulfur utilization and reduced impedance attributed to the increased electron network available for the conversion reaction. However, when the thickness of the coating layer is small (e.g., $\sim 20 \mu m$), the adsorption property of the MOF plays a more critical role in improving the battery performance. This study shows that the Li-S battery performance is highly dependent on the mass loading and thickness of the MOFbased composite membrane, as well as the ratio of each component. An optimal balance between the adsorption and conversion capabilities of the MOF-based composite layer is of great importance to reducing the mass loading and the thickness of inactive layers for high-energy-density batteries. This work suggests the importance of a holistic design consideration for a MOF-based membrane for long-life and high-energy-density Li-S batteries.

2. EXPERIMENTAL SECTION

Preparation of UiO-66-NH₂. Synthesis of UiO-66-NH₂ was performed according to a literature method with some modifications.³² Typically, ZrCl₄ (612 mg) and 2-aminoterephthalic acid (NH₂-H₂bdc) (466 mg) were dissolved in N,N-dimethylformamide (DMF) (150 mL) in a Teflon-lined reaction bottle, and the solution was sonicated for 30 min. Acetic acid (29.5 mL) and H_2O (125 μL) were added into the solution, and the mixture was heated at 120 °C for 24 h. After cooling to room temperature, the powder was collected by a centrifugation, washed with DMF and ethanol, and dried under a vacuum at 120 °C for 24 h.

Preparation of MOF/SP-Coated Separators. MOFs and SP carbon black with the desired weight ratio were manually ground for at least 15 min until the mixture showed a uniform color. The combined MOF/SP powder was mixed with polyvinylidene fluoride (PVDF) to a weight ratio of 90:10 in N-methyl-2-pyrrolidone (NMP) by a Thinky mixer. Subsequently, additional NMP solvent was added depending on the different ratios to produce a viscous slurry. The resulting slurry was cast on a Celgard 2500 separator by a doctor blade to control the coating thickness. After drying under a vacuum at 80 °C for 24 h, the coated separator was cut into a disk with a diameter of 18 mm for cell assembly or a rectangle shape of 10×25 mm for electrical conductivity measurement. The MOF/SP-coated separators were dried under a vacuum at 80 °C overnight before

Preparation of Sulfur Cathodes. Sulfur and Ketjen Black were ground with a weight ratio of 8:2 and heated at 155 °C for 12 h in a stainless-steel autoclave. After cooling, the mixture was ground again and heated at 170 °C for 12 h. The prepared sulfur/Ketjen Black, SP, and PVDF with a weight ratio of 70:15:15 were mixed and dispersed in NMP by a Thinky mixer. For making a sulfur composite cathode with MOFs, MOFs, sulfur/Ketjen Black, SP, and PVDF were mixed with a weight ratio of 15:70:15:15. The slurry was cast on carboncoated aluminum foil by a doctor blade and then dried under a vacuum at 70 °C for 4 h and overnight with the heating turned off. The electrode was cut into a disk with a diameter of 12 mm.

Lithium Polysulfide Adsorption Test. The Li₂S₆ solution was prepared by dissolving Li₂S and sulfur with a molar ratio of 1:5 in 1,3dioxolane (DOL) and 1,2-dimethoxyethane (DME) (1:1 by volume), with stirring and heating at 70 °C for 3 days. Fifteen miligrams of MOFs or SP powders were soaked in 1.5 mL of the corresponding Li₂S₆ solution in an Ar-filled glovebox, and the solutions were sealed with Teflon-lined caps and transferred out for the adsorption test.

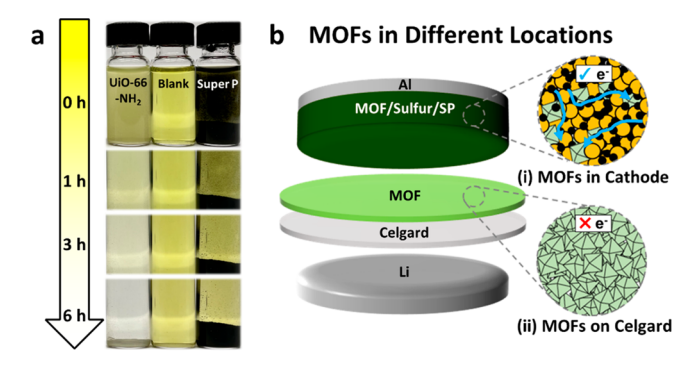
Electrochemical Testing. All electrochemical data were collected using CR-2032 type coin cells assembled in Ar-filled glovebox. Sixty microliters of 1 M lithium bis(trifluoromethane sulfonimide) (LiTFSI) with 0.2 M LiNO₃ in DOL/DME (1/1 by volume) electrolyte (1 M LiTFSI 0.2 M LiNO3 DOL/DME) was used for all cells. The galvanostatic tests were conducted on Neware cyclers, where Li-S half cells were activated at 0.1 A g⁻¹ for three cycles with the fixed voltage range at 1.8 to 2.8 V before the long-term cycling or rate capability test. Cyclic voltammetry (CV) and electrochemical impedance spectroscopy (EIS) measurements were conducted on an Autolab electrochemical workstation. The scan rate and voltage range were 0.1 mV s⁻¹ and 1.8-2.8 V with one activation cycle for the CV measurement, and the frequency range and amplitude were 1 MHz to 0.1 Hz and 0.01 V for EIS, respectively.

Material Characterization. N₂ sorption isotherms of MOFs were collected on a Micromeritics ASAP 2020 Adsorption Analyzer at 77 K. Powder X-ray diffraction (PXRD) patterns of MOFs were obtained on a Bruker D8 Advance diffractometer using Cu K α radiation. Morphologies of the MOF/SP-modified separators were obtained on a FEI Quanta 250 and Apreo scanning electron microscope (SEM). The in-plane electrical conductivity of the MOF/SP coating layer was measured by a four-probe method with a Keithley 2400.

3. RESULTS AND DISCUSSION

LiPS Adsorption Property and Trapping Effect of MOFs in Coin Cells. Considering its high porosity, electrochemical stability, and polar functional group (Figures S1 and S2), UiO-66-NH2 was selected as a model MOF material to study its trapping effect on cell stability.³² To evaluate the interaction between MOFs and LiPS species, we conducted a LiPS adsorption test by soaking an equal weight of UiO-66-NH₂ or SP powders into 1 mM Li₂S₆ in DOL/DME (1/1 by volume) (Figure 1a). After 6 h, the UiO-66-NH₂-soaked solution became nearly transparent, which can be attributed to the adsorption of Li₂S₆ into MOF pores, driven by the trapping effect of nanopores and its interaction with the polar functional groups (-NH₂).^{33,34} By contrast, the SP-soaked solution showed no noticeable difference compared to the blank solution (1 mM Li₂S₆ in DOL/DME), indicating a weak adsorption ability of SP toward LiPS species.

To better understand how the LiPS adsorption property of MOFs influences the performance of Li-S batteries, MOFs were installed in two different locations inside a coin cell: (i) inside a sulfur cathode and (ii) on a Celgard separator (Figure 1b). By placing MOFs on the Celgard separator, MOFs can be expected to effectively adsorb or trap LiPS species that diffuse across the separator. On the other hand, by adding MOFs inside the sulfur cathode, the MOFs can be expected to adsorb LiPS formed during the redox reaction and reutilize LiPS by taking advantage of the electrically conductive nature of cathode formed by SP. Li-S half cells were assembled and cycled at 0.5 A g⁻¹ with 1 M LiTFSI 0.2 M LiNO₃ DOL/DME (Figure 1c). The cell with MOFs on Celgard delivers a slightly higher capacity for the first 80 cycles compared to pristine Celgard, but capacity starts to fade even lower than the pristine Celgard after 80 cycles. However, the cell with MOFs in the sulfur cathode gives better capacity retention and higher capacities than both pristine Celgard or MOF-coated Celgard for more than 100 cycles. The different trends in capacity decay by placing MOFs in different locations of the cell implies that introducing MOFs into electron pathways could be more important than solely blocking the migration of LiPS to the anode side.



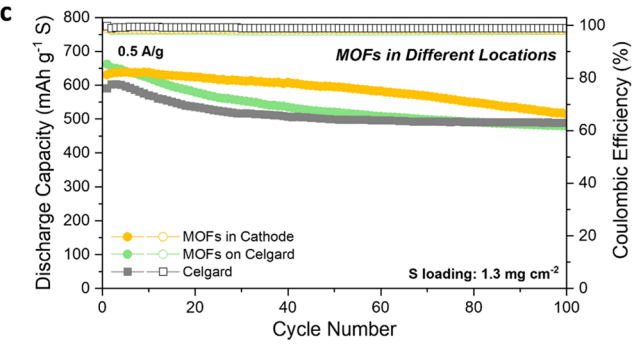


Figure 1. (a) Optical photographs showing the LiPS adsorption test of UiO-66-NH₂ and SP in 1 mM Li₂S₆ DOL/DME (1/1 by volume). (b) Schematic showing two types of coin cell configurations by placing MOFs in different locations: (i) MOFs in a sulfur cathode and (ii) MOFs on a Celgard separator. (c) Discharge capacity and Coulombic efficiency of Li–S half cells with MOFs in different locations in the cell.

Effect of Electrical Conductivity of MOF/SP Separator on Cycling Performance. To further understand the importance of the electron pathway connected to MOF particles, we systematically adjusted the electrical conductivity of MOF-based separators by changing the ratio between MOFs and SP in the coating layer (Figure 2a). The SP was chosen as the conductive material in the coating layer because it was also used as conductive additive in the cathode. The top and cross-sectional scanning electron microscopy (SEM) images (Figure S3) show a uniform mixture of MOFs and SP in the coating layer and similar coating thicknesses (~40 μ m) of composite layers with different MOF to SP ratios. Optical and SEM images of the backside of MOF/SP-modified Celgard membranes show no penetration of MOFs or SP particles through the membrane (Figure S4), indicating that the electrically insulating function of the separator is maintained after modifying one side with electrically conductive material. Table S1 shows the thickness and mass loading data of modified separators used in this work as well as a description of the experimental design. As expected, the trend in electrical conductivity of the MOF/SP layer follows the increased SP content in the layer, where higher SP content results in higher electrical conductivity for the MOF/SP composite (Figure 2b). The pure MOF-coated layer (denoted as MOF/SP 90/0 based on 90 wt% MOF, 0 wt% SP, and 10 wt % PVDF) presents electrical conductivity of 2.3×10^{-7} S cm⁻¹ with a slightly higher value of 1.9×10^{-6} S cm⁻¹ obtained for MOF/SP 80/10. The pure SP-coated layer (MOF/SP 0/90) shows a high electrical conductivity of 5.5 S cm⁻¹, and the equal mass mixture (MOF/SP 45/45) gives a comparable electrical conductivity (3.8 S cm⁻¹).

To demonstrate how different electrical conductivity influences the performance of Li-S batteries, we assembled half cells with sulfur cathodes (1.3 mg cm⁻²) and 1 M LiTFSI 0.2 M LiNO₃ DOL/DME electrolyte by using the MOF/SPmodified Celgard membrane as the separator and a pristine Celgard membrane as the control. The initial capacities at 0.5 A g⁻¹ (Figure 2c) are 590, 662, 714, 975, and 1084 mAh g⁻¹ (based on S mass) for the cells with Celgard, MOF/SP 90/0, 80/10, 45/45, and 0/90, respectively. The increased initial capacity with the increased SP content in the coating layer can be explained by the increased sulfur utilization from the conductive carbon.³⁵ Because of the intimate contact between the cathode and MOF/SP coating layer, the electrically conductive layer can promote the efficient utilization of sulfur. Moreover, the improved performance with more SP content indicates that the coating layer can work as a secondary current collector. The dissolved LiPS species could be trapped by the coating layer. Because the coating layer is in contact with the cathode layer that is already electrically conductive, the coating layer and cathode layer can have an electrical connection, which will provide an electron pathway to reutilize the trapped LiPS in the coating layer (Figure 2a). Because the electrical conductivity of the secondary current collector determines how effective LiPS species can be utilized, the initial capacity and capacity retention hugely depend on the electrical conductivity of the coating layer. In addition, the rate capability was conducted (Figure 2d). At all rates, the modified separators with more SP content gave higher capacity and Coulombic efficiency, highlighting the importance of electrical conductivity of the coating layer at different rates.

Furthermore, to decouple the effect of electrical conductivity and the adsorption capability, another layer of Celgard membrane was placed between the cathode and MOF/SP composite layer (Figure 2e). The additional separator layer electrically insulates the MOF/SP composite layer, disabling its function as a secondary current collector. Both the capacities of Li-S cells with MOF/SP 45/45 and 0/90 significantly decreased after electrically isolating the composite layer (Figure 2c, f), confirming that the performance enhancement of the MOF-based composite is mainly a result of electrical conduction. In addition, the lower capacities of MOF 45/45 compared to 0/90 can be attributed to the continuous LiPS adsorption by MOF particles that form isolated (inactive) LiPS. These results clearly show that electrical conductivity of the composite layer is strongly correlated with the Li-S battery performance.

Electrochemical Analysis of MOF/SP Separator. To better understand the electrochemical properties of the MOF/ SP-modified separators, we analyzed voltage profiles, CV, and EIS. The voltage profiles at different charge/discharge rates show the increase in overpotential with the decrease in electrical conductivity of the coating layer (Figure S5). At 0.1 A g^{-1} (Figure 3a), the second discharge plateau (\sim 2.1 V) remains similar for all separators and a slight increase in the charge plateau with the decrease in SP content. At a higher rate of 1 A g⁻¹ (Figure 3b), the second discharge plateau of the pure MOF-modified separator (MOF/SP 90/0) decreased to \sim 2.05 V, and the charge plateau increased higher. At 3 A g⁻¹ (Figure 3c), the increase in overpotential with a decrease in SP content is even more obvious in addition to significantly decreased capacity. This trend indicates that not only the initial capacity and capacity retention but also redox kinetics largely depend on the electrical conductivity of the coating layer.

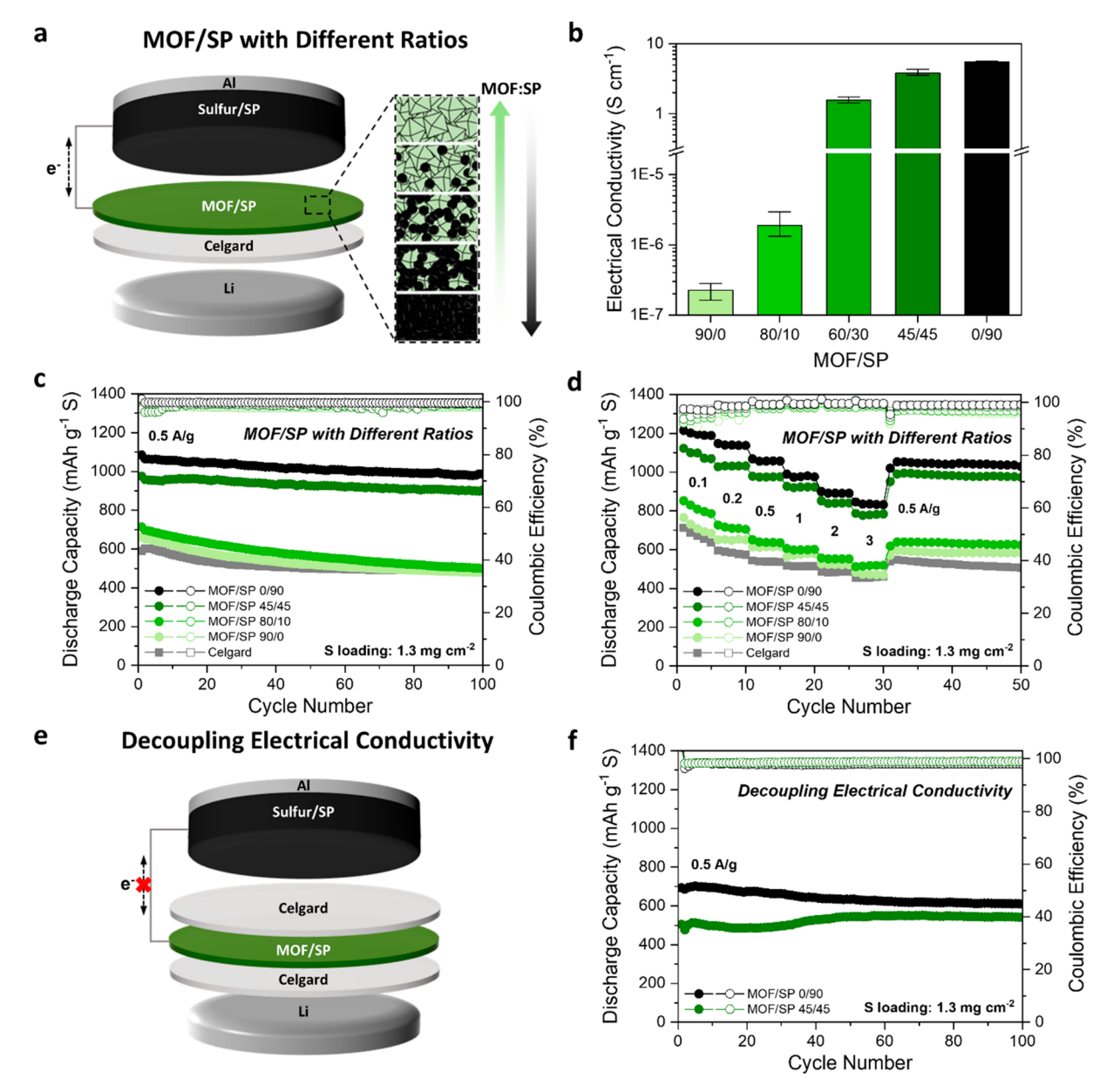


Figure 2. (a) Scheme and (b) electrical conductivity of MOF/SP-modified separators with different ratios. (c) Cycling performance and (d) rate capability of MOF/SP-modified separators with Coulombic efficiency. (e) Scheme and (f) cycling performance of electrically insulated MOF/SP-modified separator by adding one layer of Celgard membrane between the cathode and the MOF/SP layer.

A CV test was conducted with half cells with the same mass loading at a scan rate of 0.1 mV s⁻¹ (Figure 3d). In general, two reduction and two oxidation peaks are observed, in which the higher reduction peak (~2.3 V) corresponds to the conversion of S_8 to Li_2S_n (4 $\leq n \leq 8$), and the lower peak (~2.0 V) corresponds to Li_2S_n (4 \le n \le 8) to $\text{Li}_2S/\text{Li}_2S_2$. 36 The reduction peaks show a positive shift, and the oxidation peaks show a negative shift with the increase of the SP content, which indicates the reduced polarization due to the increased electron pathway available to active sulfur species. Also, the increase in specific current with more SP content indicates the more utilization of sulfur species, and the stable peaks of the modified separators in full CV profiles (Figure S6) show stable cycling of the modified separators. The EIS data of half cells were collected before (Figure S7) and after 20 cycles (Figure 3e). After 20 cycles, it shows that the electrode charge-transfer impedance decreased with increased SP content, where MOF/

SP 90/0, 80/10, 45/45, and 0/90 have 16, 13, 7, and 4 Ω , respectively. The reduced impedance and increased utilization of sulfur can be ascribed to higher electrical conductivity of the coating layer, which facilitates the charge transfer of redox reaction with sulfur species.

To understand the behavior of the MOF/SP-coated separators with increased sulfur content, we assembled half cells with high sulfur loading cathodes (3.5 mg cm⁻²) by using MOF/SP with 45/45 and 0/90 ratios (Figure S8). The initial capacities were 888, 936, and 446 mAh g⁻¹ for cells with MOF/SP 45/45, MOF/SP 0/90, and the pristine Celgard membrane, respectively. The superior performance of the pure SP-modified separator can be attributed to the better sulfur utilization in thick cathodes. Since the high sulfur loading cathodes suffer from the low utilization of sulfur because of an insufficient electron pathway, the high electrical conductivity of the modified separator dominates the performance. On the

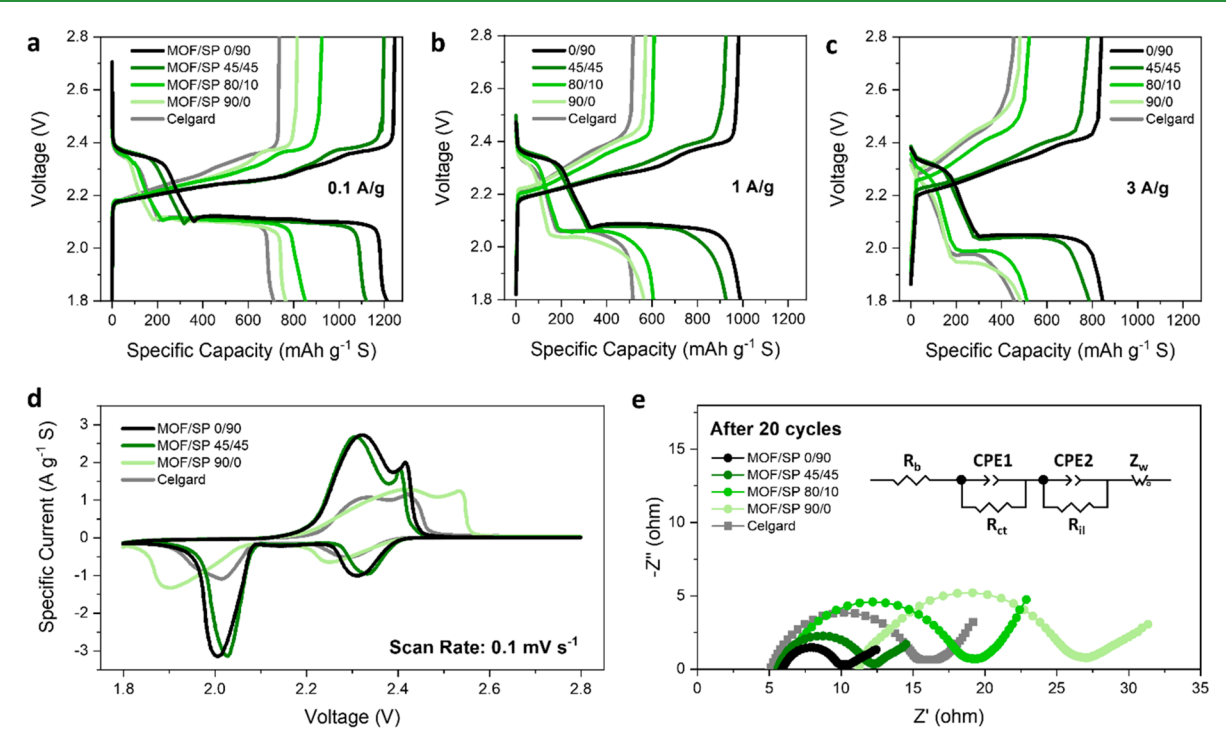


Figure 3. First charge/discharge profiles at (a) 0.1, (b) 1, and (c) 3 A/g. (d) CV profiles and (e) EIS of Li-S half cells using MOF/SP-modified separators with different MOF to SP ratios and the corresponding equivalent circuit.

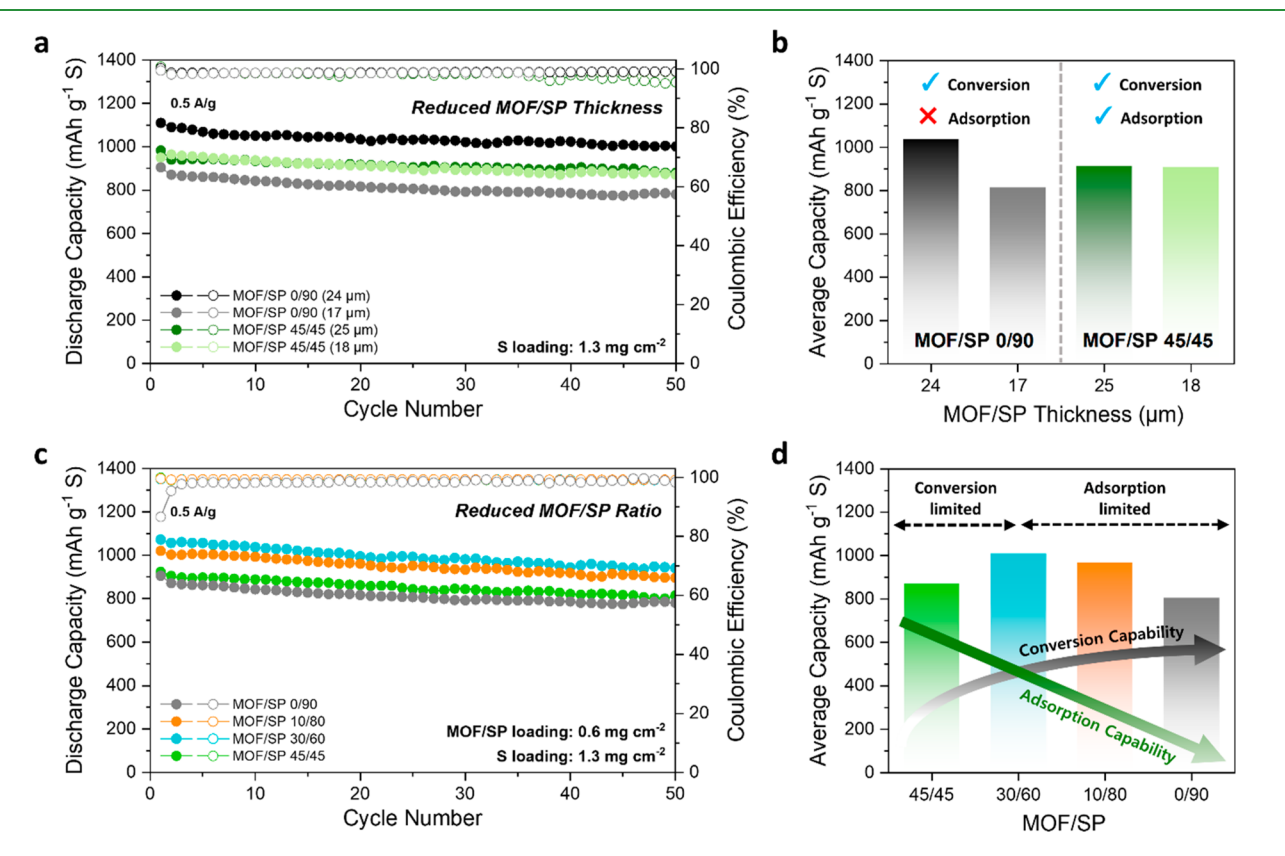


Figure 4. Discharge capacity, Coulombic efficiency, and average discharge capacity of Li–S half cells with MOF/SP-coated separators with (a, b) reduced MOF/SP thickness and (c, d) reduced MOF/SP ratio with fixed MOF/SP loading (0.6 mg cm⁻²).

basis of the above results, it would appear that the superior performance of the pure SP-modified separator renders MOFs not a critical functional component. However, a relatively thick coating layer (\sim 40 μ m) was deliberately used in our earlier

experiments to demonstrate the relation between electrical conductivity and the performance of the modified separators.

Effect of the Thickness and MOF Loading of the MOF/SP Layer. For practical application, it is necessary to

have the coating layer as light and thin as possible because additional thickness is dead weight that eventually decreases the gravimetric and volumetric energy densities of batteries.³⁷ To achieve the highest possible energy density, we prepared thinner layers of MOF/SP 45/45 and 0/90 modified separators, and their thicknesses were verified by crosssectional SEM images (Figure S9). MOF/SP 45/45 was prepared with coating thicknesses of 25 and 18 μ m, whereas MOF/SP 0/90 was prepared with coating thicknesses of 24 and 17 μ m. With such thin modified separators, Li-S half cells were assembled and cycled at 0.5 A g⁻¹ (Figure 4a). For MOF/SP 45/45, the average capacities remained similar for the 25 and 18 μ m (914 and 907 mAh g⁻¹, respectively) (Figure 4b). By comparison, for MOF/SP 0/90, the average capacity of the cell with a 17 μ m coating layer was significantly lower than that of 24 μ m (813 and 1035 mAh g⁻¹, respectively). This flipped trend between MOF/SP 45/45 and 0/90 can be explained by the synergetic effects of adsorption (attributed to the MOF porous structure) and conversion (associated with the electrical conductivity) of LiPS species. For the separators with both LiPS adsorption and conversion capabilities (e.g., MOF/SP 45/45), despite the shorter diffusion length (small membrane thickness), MOFs adsorb LiPS species to prevent the loss of LiPS species, whereas the electron pathway of SP enables the reutilization of the trapped LiPS species. However, for the separators with a strong conversion capability but weak adsorption capability (e.g., MOF/SP 0/90), the diffusion length solely determines the degree of LiPS utilization for the reaction, and thus the decrease in thickness significantly deteriorates the performance.

After understanding the synergetic effects of adsorption and conversion at limited diffusion length of composite layers, these two counterbalancing capabilities were further investigated by reducing the MOF/SP ratios while fixing the mass loading of the composite layer. Because a noticeable capacity drop was observed for MOF/SP 45/45 at a reduced composite loading (below 0.6 mg cm⁻²) (Figure S10), half cells were assembled using lower MOF ratios with a fixed composite loading of 0.6 mg cm⁻² (Figure 4c). It was observed that increasing the conversion capability (MOF/SP 45/45 and 30/ 60) gives higher average capacities (871 and 1008 mAh g⁻¹, respectively), whereas a further increase (MOF/SP 10/80 and 0/90) lowers the capacities (966 and 802 mAh g⁻¹, respectively) (Figure 4d). This trend indicates that conversion is limited for MOF/SP 45/45 and adsorption is limited for MOF/SP 10/80 and 0/90 based on the highest average discharge capacity for MOF/SP 30/60. This result indicates that an optimal balance between the adsorption and conversion capabilities in a thin composite layer is necessary to achieve both high capacity and stable cycling performance without obviously increasing the inactive components. In addition, to understand the practical aspect of the optimized composite membrane, which has a thickness of around 10 μ m (Figure S11), we projected the stack energy density with different thicknesses of the MOF/SP 30/60 composite layer (Figure S12 and Table S2).³⁸ It was shown that reducing the composite thickness from 100 to 10 μ m significantly increases the stack energy density, while further reducing to 1 μ m has a minimal increase, confirming the feasibility of the composite membrane for practical application.

4. CONCLUSIONS

In summary, we show a different perspective of understanding the property-performance relation of MOF/SP-modified separators in Li-S batteries by adjusting the MOF/SP ratio, thickness, and mass loading of the composite. The electrochemical results show that the modified layers with higher electrical conductivity have significantly improved performance, thereby decreasing the impedance and overpotential at various charge/discharge rates. On the other hand, LiPS adsorption becomes crucial when the diffusion length is limited (i.e., reduced composite thickness) and electrical conductivity is saturated (i.e., reduced MOF loading). For future applications, an optimal balance between the adsorption and conversion capabilities of a thin and light composite layer is necessary to achieve a long life and the highest energy density. This work aims to clarify the synergetic effects between the LiPS adsorption property of MOFs and the conversion property of conductive materials of the modified separators in Li-S batteries, thus providing a better understanding on the role of MOFs in such modified separators.

ASSOCIATED CONTENT

5 Supporting Information

The Supporting Information is available free of charge at https://pubs.acs.org/doi/10.1021/acsami.2c08404.

N₂ sorption, PXRD pattern, SEM images, voltage and CV profiles, EIS data, high sulfur loading and reduced MOF/SP loading performance, energy density projections, summary table of thickness, mass loading and description of experimental design, and parameters used for the energy density projections (PDF)

AUTHOR INFORMATION

Corresponding Authors

Zheng Chen — Department of NanoEngineering, Program of Materials Science, Program of Chemical Engineering, and Sustainable Power and Energy Center, University of California, San Diego, La Jolla, California 92093, United States; ocid.org/0000-0002-9186-4298; Email: zhengchen@eng.ucsd.edu

Guorui Cai — Department of NanoEngineering, University of California, San Diego, La Jolla, California 92093, United States; Email: gcai@eng.ucsd.edu

Authors

Dong Ju Lee – Department of NanoEngineering, University of California, San Diego, La Jolla, California 92093, United States

Xiaolu Yu — Program of Materials Science, University of California, San Diego, La Jolla, California 92093, United States

R. Eric Sikma – Department of Chemistry and Biochemistry, University of California, San Diego, La Jolla, California 92093, United States; orcid.org/0000-0002-5313-661X

Mingqian Li — Program of Chemical Engineering, University of California, San Diego, La Jolla, California 92093, United States

Seth M. Cohen – Department of NanoEngineering and Department of Chemistry and Biochemistry, University of California, San Diego, La Jolla, California 92093, United States; orcid.org/0000-0002-5233-2280

Complete contact information is available at:

https://pubs.acs.org/10.1021/acsami.2c08404

Author Contributions

G.C. and Z.C. conceived the original idea and designed the expirement. Z. C. directed the project. D.L. carried out the experiments. D.L. and X.Y. synthesized the material. R.E.S. and M.L. assisted with characterization. D.L., G.C., Z.C., and S.M.C wrote the paper. All authors discussed the results and commented on the manuscript.

Notes

The authors declare no competing financial interest.

ACKNOWLEDGMENTS

This work was supported by the National Science Foundation through the U.C. San Diego Materials Research Science and Engineering Center (UCSD MRSEC, DMR-2011924). This work was performed in part at the San Diego Nanotechnology Infrastructure (SDNI) of U.C. San Diego, a member of the National Nanotechnology Coordinated Infrastructure, which is supported by the National Science Foundation (Grant ECCS-1542148). This work (MOF characterization) was also supported in part by a grant from the Department of Energy, Office of Basic Energy Sciences, Division of Materials Science and Engineering, under Award DE-FG02-08ER46519.

REFERENCES

- (1) Zhao, C.; Xu, G.-L.; Yu, Z.; Zhang, L.; Hwang, I.; Mo, Y.-X.; Ren, Y.; Cheng, L.; Sun, C.-J.; Ren, Y.; et al. A High-Energy and Long-Cycling Lithium—Sulfur Pouch Cell via a Macroporous Catalytic Cathode With Double-End Binding Sites. *Nat. Nanotechnol.* **2021**, *16* (2), 166–173.
- (2) Liu, D.; Zhang, C.; Zhou, G.; Lv, W.; Ling, G.; Zhi, L.; Yang, Q. H. Catalytic Effects in Lithium—Sulfur Batteries: Promoted Sulfur Transformation and Reduced Shuttle Effect. *Adv. Sci.* **2018**, *5* (1), 1700270.
- (3) Lim, W. G.; Kim, S.; Jo, C.; Lee, J. A Comprehensive Review of Materials With Catalytic Effects in Li-S Batteries: Enhanced Redox Kinetics. *Angew. Chem., Int. Ed.* **2019**, *58* (52), 18746–18757.
- (4) Pang, Q.; Liang, X.; Kwok, C. Y.; Nazar, L. F. Advances in Lithium–Sulfur Batteries Based on Multifunctional Cathodes and Electrolytes. *Nat. Energy* **2016**, *1*, 16132.
- (5) Safari, M.; Kwok, C.; Nazar, L. Transport Properties of Polysulfide Species in Lithium—Sulfur Battery Electrolytes: Coupling of Experiment and Theory. ACS Cent. Sci. 2016, 2 (8), 560–568.
- (6) Li, G.; Lei, W.; Luo, D.; Deng, Y.; Deng, Z.; Wang, D.; Yu, A.; Chen, Z. Stringed "Tube on Cube" Nanohybrids As Compact Cathode Matrix for High-Loading and Lean-Electrolyte Lithium—Sulfur Batteries. *Energy Environ. Sci.* **2018**, *11* (9), 2372–2381.
- (7) Li, G.; Wang, S.; Zhang, Y.; Li, M.; Chen, Z.; Lu, J. Revisiting the Role of Polysulfides in Lithium—Sulfur Batteries. *Adv. Mater.* **2018**, *30* (22), 1705590.
- (8) Zhang, G.; Peng, H. J.; Zhao, C. Z.; Chen, X.; Zhao, L. D.; Li, P.; Huang, J. Q.; Zhang, Q. The Radical Pathway Based on a Lithium-Metal-Compatible High-Dielectric Electrolyte for Lithium-Sulfur Batteries. *Angew. Chem., Int. Ed.* **2018**, *57*, 16732–16736.
- (9) Zhong, Y.; Yin, L.; He, P.; Liu, W.; Wu, Z.; Wang, H. Surface Chemistry in Cobalt Phosphide-Stabilized Lithium—Sulfur Batteries. *J. Am. Chem. Soc.* **2018**, *140* (4), 1455–1459.
- (10) Xu, R.; Li, J. C.; Lu, J.; Amine, K.; Belharouak, I. Demonstration of Highly Efficient Lithium—Sulfur Batteries. *J. Mater. Chem. A* **2015**, 3 (8), 4170–4179.
- (11) Zhang, J.; Li, Z.; Chen, Y.; Gao, S.; Lou, X. W. Nickel—Iron Layered Double Hydroxide Hollow Polyhedrons as a Superior Sulfur Host for Lithium—Sulfur Batteries. *Angew. Chem., Int. Ed.* **2018**, *57*, 10944—10948.

- (12) Yang, Z.; Peng, C.; Meng, R.; Zu, L.; Feng, Y.; Chen, B.; Mi, Y.; Zhang, C.; Yang, J. Hybrid Anatase/Rutile Nanodots-Embedded Covalent Organic Frameworks With Complementary Polysulfide Adsorption for High-Performance Lithium—Sulfur Batteries. *ACS Cent. Sci.* **2019**, *5*, 1876—1883.
- (13) Chen, H.; Zhou, G.; Boyle, D.; Wan, J.; Wang, H.; Lin, D.; Mackanic, D.; Zhang, Z.; Kim, S. C.; Lee, H. R.; et al. Electrode Design With Integration of High Tortuosity and Sulfur-Philicity for High-Performance Lithium-Sulfur Battery. *Matter* **2020**, 2 (6), 1605—1620.
- (14) Jin, Z.; Lin, T.; Jia, H.; Liu, B.; Zhang, Q.; Li, L.; Zhang, L.; Su, Z.-m.; Wang, C. Expediting the Conversion of Li_2S_2 to Li_2S Enables High-Performance Li–S Batteries. *ACS Nano* **2021**, *15* (4), 7318–7327.
- (15) Jiang, H.; Liu, X. C.; Wu, Y.; Shu, Y.; Gong, X.; Ke, F. S.; Deng, H. Metal—Organic Frameworks for High Charge—Discharge Rates in Lithium—Sulfur Batteries. *Angew. Chem., Int. Ed.* **2018**, *57*, 3916—3921.
- (16) Kim, S. H.; Yeon, J. S.; Kim, R.; Choi, K. M.; Park, H. S. A Functional Separator Coated With Sulfonated Metal-Organic Framework/Nafion Hybrids for Li-S Batteries. *J. Mater. Chem. A* **2018**, *6* (48), 24971–24978.
- (17) Han, D.-D.; Wang, Z.-Y.; Pan, G.-L.; Gao, X.-P. Metal—Organic-Framework-Based Gel Polymer Electrolyte With Immobilized Anions To Stabilize a Lithium Anode for a Quasi-Solid-State Lithium—Sulfur Battery. ACS Appl. Mater. Interfaces 2019, 11 (20), 18427—18435.
- (18) Tian, M.; Pei, F.; Yao, M.; Fu, Z.; Lin, L.; Wu, G.; Xu, G.; Kitagawa, H.; Fang, X. Ultrathin MOF Nanosheet Assembled Highly Oriented Microporous Membrane as an Interlayer for Lithium-Sulfur Batteries. *Energy Storage Mater.* **2019**, *21*, 14–21.
- (19) Cai, G.; Yan, P.; Zhang, L.; Zhou, H.-C.; Jiang, H.-L. Metal—Organic Framework-Based Hierarchically Porous Materials: Synthesis and Applications. *Chem. Rev.* **2021**, *121*, 12278–12326.
- (20) Cai, G.; Yin, Y.; Xia, D.; Chen, A. A.; Holoubek, J.; Scharf, J.; Yang, Y.; Koh, K. H.; Li, M.; Davies, D. M.; et al. Sub-Nanometer Confinement Enables Facile Condensation of Gas Electrolyte for Low-Temperature Batteries. *Nat. Commun.* **2021**, *12*, 3395.
- (21) Han, J.; Gao, S.; Wang, R.; Wang, K.; Jiang, M.; Yan, J.; Jin, Q.; Jiang, K. Investigation of the Mechanism of Metal—Organic Frameworks Preventing Polysulfide Shuttling From the Perspective of Composition and Structure. *J. Mater. Chem. A* **2020**, 8 (14), 6661–6669.
- (22) Qi, C.; Xu, L.; Wang, J.; Li, H.; Zhao, C.; Wang, L.; Liu, T. Titanium-Containing Metal—Organic Framework Modified Separator for Advanced Lithium—Sulfur Batteries. *ACS Sustain. Chem. Eng.* **2020**, *8* (34), 12968—12975.
- (23) Bai, S.; Liu, X.; Zhu, K.; Wu, S.; Zhou, H. Metal—Organic Framework-Based Separator for Lithium—Sulfur Batteries. *Nat. Energy* **2016**, *1*, 16094.
- (24) Yuan, N.; Sun, W.; Yang, J.; Gong, X.; Liu, R. Multifunctional MOF-Based Separator Materials for Advanced Lithium-Sulfur Batteries. *Adv. Mater. Interfaces* **2021**, 8 (9), 2001941.
- (25) Zhu, D.; Long, T.; Xu, B.; Zhao, Y.; Hong, H.; Liu, R.; Meng, F.; Liu, J. Recent Advances in Interlayer and Separator Engineering for Lithium-Sulfur Batteries. *J. Energy Chem.* **2021**, *57*, 41–60.
- (26) He, Y.; Chang, Z.; Wu, S.; Qiao, Y.; Bai, S.; Jiang, K.; He, P.; Zhou, H. Simultaneously Inhibiting Lithium Dendrites Growth and Polysulfides Shuttle by a Flexible MOF-Based Membrane in Li—S Batteries. *Adv. Energy Mater.* **2018**, *8* (34), 1802130.
- (27) Lee, D. H.; Ahn, J. H.; Park, M.-S.; Eftekhari, A.; Kim, D.-W. Metal-Organic Framework/Carbon Nanotube-Coated Polyethylene Separator for Improving the Cycling Performance of Lithium-Sulfur Cells. *Electrochim. Acta* **2018**, 283, 1291–1299.
- (28) Fan, Y.; Niu, Z.; Zhang, F.; Zhang, R.; Zhao, Y.; Lu, G. Suppressing the Shuttle Effect in Lithium—Sulfur Batteries by a UiO-66-Modified Polypropylene Separator. *ACS Omega* **2019**, 4 (6), 10328–10335.

- (29) Wang, X.; Zhao, Y.; Wu, F.; Liu, S.; Zhang, Z.; Tan, Z.; Du, X.; Li, J. ZIF-7@Carbon Composites as Multifunctional Interlayer for Rapid and Durable Li-S Performance. J. Energy Chem. 2021, 57, 19-
- (30) Zheng, S.; Zhao, X.; Liu, G.; Wu, F.; Li, J. A Multifunctional UiO-66@Carbon Interlayer as an Efficacious Suppressor of Polysulfide Shuttling for Lithium-Sulfur Batteries. Nanotechnology 2021, 32, 365404.
- (31) Guo, S.; Xiao, Y.; Wang, J.; Ouyang, Y.; Li, X.; Deng, H.; He, W.; Zeng, Q.; Zhang, W.; Zhang, Q.; Huang, S. Ordered Structure of Interlayer Constructed With Metal-Organic Frameworks Improves the Performance of Lithium-Sulfur Batteries. Nano Research 2021, 14, 4556-4562.
- (32) Cai, G.; Ma, X.; Kassymova, M.; Sun, K.; Ding, M.; Jiang, H.-L. Large-Scale Production of Hierarchically Porous Metal-Organic Frameworks by a Reflux-Assisted Post-synthetic Ligand Substitution Strategy. ACS Cent. Sci. 2021, 7 (8), 1434-1440.
- (33) Li, S.; Lin, J.; Ding, Y.; Xu, P.; Guo, X.; Xiong, W.; Wu, D.-Y.; Dong, Q.; Chen, J.; Zhang, L. Defects Engineering of Lightweight Metal-Organic Frameworks-Based Electrocatalytic Membrane for High-Loading Lithium-Sulfur Batteries. ACS Nano 2021, 15 (8), 13803-13813.
- (34) Suriyakumar, S.; Stephan, A. M.; Angulakshmi, N.; Hassan, M. H.; Alkordi, M. H. Metal-Organic framework@SiO2 as Permselective Separator for Lithium-Sulfur Batteries. J. Mater. Chem. A 2018, 6 (30), 14623-14632.
- (35) Brückner, J.; Thieme, S.; Grossmann, H. T.; Dörfler, S.; Althues, H.; Kaskel, S. Lithium-Sulfur Batteries: Influence of C-Rate, Amount of Electrolyte and Sulfur Loading on Cycle Performance. J. Power Sources 2014, 268, 82-87.
- (36) Hong, X.-J.; Song, C.-L.; Yang, Y.; Tan, H.-C.; Li, G.-H.; Cai, Y.-P.; Wang, H. Cerium Based Metal-Organic Frameworks as an Efficient Separator Coating Catalyzing the Conversion of Polysulfides for High Performance Lithium-Sulfur Batteries. ACS Nano 2019, 13 (2), 1923-1931.
- (37) Chung, S. H.; Chang, C. H.; Manthiram, A. Progress on the Critical Parameters for Lithium-Sulfur Batteries to Be Practically Viable. Adv. Funct. Mater. 2018, 28 (28), 1801188.
- (38) Betz, J.; Bieker, G.; Meister, P.; Placke, T.; Winter, M.; Schmuch, R. Theoretical versus Practical Energy: A Plea for More Transparency in the Energy Calculation of Different Rechargeable Battery Systems. Adv. Energy. Mater. 2019, 9 (6), 1803170.

□ Recommended by ACS

Highly Efficient Polysulfide Trapping and Ion Transferring within a Hierarchical Porous Membrane Interlayer for High-**Energy Lithium-Sulfur Batteries**

Shuting Wang, Gaohong He, et al.

APRIL 24, 2020

ACS APPLIED ENERGY MATERIALS

RFAD 🗹

Immobilization and Kinetic Acceleration of Lithium Polysulfides by Iodine-Doped MXene Nanosheets in **Lithium-Sulfur Batteries**

Wenbin Yu, Pengjian Zuo, et al.

IUNF 29 2022

THE JOURNAL OF PHYSICAL CHEMISTRY C

READ **C**

Metal-Organic Framework Decorated Polymer Nanofiber Composite Separator for Physiochemically Shielding Polysulfides in Stable Lithium-Sulfur Batteries

Shujun Zheng, Yi Xie, et al.

AUGUST 05, 2021 **ENERGY & FUELS**

RFAD 17

Novel Interlayer on the Separator with the Cr₃C₂ Compound as a Robust Polysulfide Anchor for Lithium-Sulfur Batteries

Xiaohong Liu, Xingtao Xu, et al.

MARCH 19, 2020

INDUSTRIAL & ENGINEERING CHEMISTRY RESEARCH

RFAD 🗹

Get More Suggestions >